Multibody Syst Dyn
https://doi.org/10.1007/s11044-020-09748-8

Effect of applied force cosimulation schemes on recoupled vehicle/track problems

Bryan Olivier[1] · **Olivier Verlinden**[1] · **Georges Kouroussis**[1]

Received: 22 January 2020 / Accepted: 27 May 2020

Abstract The aim of this paper is to discuss the effect of cosimulation on a railway vehicle/track/soil model. Firstly, only the vehicle and a flexible track are considered without taking the soil flexibility into account. Two well-known co-simulation approaches are used: a parallel approach, called Jacobi, and a sequential approach, called Gauß–Seidel. The definition of the subsystems, thus the place at which the entire system is split, is discussed. For the vehicle/track case, the split can be performed either between the wheel and the rail or between the rail and the sleepers. Moreover, it is shown that the output of each subsystem, either a kinematic quantity or a force, has a significant impact on the results since. It is indeed observed that, for the vehicle/track model, exchanging only kinematic quantities between the subsystem is less accurate but more stable than exchanging forces and kinematic quantities. The macrotimestep influence is also investigated and it is demonstrated that when the macrotimestep decreases, all co-simulation configuration converge to the same solution. Secondly, the soil flexibility and the vehicle influences are considered with a vehicle/track/soil model involving two different software environments: a multibody dedicated program for the vehicle and the track and a finite element analysis program for the soil. Generally, a deterioration of the results is observed in soft soil cases.

Keywords Solver-coupling · Cosimulation · Railway dynamics · Finite element analysis

1 Introduction

The ground-borne vibrations generated by a train moving along a track on a flexible soil can cause discomfort or environmental nuisances in surrounding buildings [1]. Therefore it be-

✉ B. Olivier
bryan.olivier@umons.ac.be

O. Verlinden
olivier.verlinden@umons.ac.be

G. Kouroussis
georges.kouroussis@umons.ac.be

[1] Department of Theoretical Mechanics, Dynamics and Vibrations, Faculty of Engineering, University of Mons, Place du Parc 20, 7000 Mons, Belgium

comes useful to estimate those vibrations in order to take relevant measures to prevent those nuisances [2]. To predict ground vibrations, finite element analyses represent nowadays an interesting alternative to frequency/wavenumber numerical approaches due to the easy way to model complex geometry and incorporating advanced mechanical behavior. In addition, time domain simulations offer the possibility to include nonlinearities. Recent works also demonstrated the utility of including a detailed model of the vehicle in the simulation to faithfully take into account the dynamic interaction between the vehicle and the track when geometrical irregularities exist at the wheel/rail contact [3, 4].

Dedicated software packages are thus necessary to model the whole vehicle/track/soil system. However, such packages are usually adapted to specific subsystems: the multibody approach for the vehicle subsystem, the finite element approach for the track and the soil systems. Although coupling the track system with the vehicle subsystem is not complicated [5, 6], adding the soil subsystem is challenging. To circumvent the problem, two-step numerical models were recently proposed to get the best of different simulation environments [7]. The idea behind this approach is to separate the whole system into several subdomains (usually 2 subdomains), and thus neglecting their dynamic interaction. Most of these models neglect the vehicle/track interaction, by presenting a single track/soil model considering the vehicle as a sequence of axle load (moving load models). Such models are relatively accurate when the dynamic interaction between the vehicle and the track is low. Typically, railway-induced vibrations by high-speed train are covered by this category if rail unevenness is neglected (e.g., [8]). Other approaches consider the decoupling in the track, either on the railpad [2] or on the ballast [9]. However, this decoupling can be unadapted in certain cases as for soft soils [10]. Therefore, this paper investigates some co-simulation implementations for the vehicle/track/soil system.

The modeling of vehicle/track interaction using co-simulation was already discussed in the literature. Antunes et al. [11] establish a three-dimensional modeling of the vehicle and the track recoupled at the wheel/rail contact. This modeling allows therefore the consideration of lateral dynamics in either straight or curved tracks. Moreover, in the proposed coupling, the vehicle subsystem receives a force quantity while the track inputs are the kinematic quantities corresponding to the motion of the vehicle wheels. Wu et al. [12, 13] also proposed a similar recoupling of the vehicle/track system with an additional layer in the track modeling which allows a more accurate representation of the subgrade. Dietz et al. [14] also studied the coupling between vehicles and tracks using cosimulation between a vehicle modeled using a multibody approach while the track is modeled using finite elements. In this model, the track is modally reduced to avoid a too large computational burden. The aforementioned models are mainly focused on the vehicle/track dynamics without modeling properly the soil. Therefore, the advantage of the model used in this paper is to investigate the different coupling techniques allowed while a more comprehensive modeling of the soil is taken into account.

Firstly, the soil is discarded and a model is built to simulate the passage of a vehicle on a track laying on a rigid foundation. The vehicle model is constructed according to the multibody approach (minimal coordinates) while the track is represented by a two-dimensional finite element model. Both vehicle and track equations are time-integrated in the same program which includes built-in cosimulation routines. An advantage of this simple model is the availability of a monolithic solution. It is therefore used to analyze the influence of cosimulation approaches (Jacobi or Gauß–Seidel, coupling types (displacement–displacement X–X or displacement–force X–T) and split location (wheel/rail W/R and rail/sleepers R/S) illustrated in Fig. 1.

Secondly, the soil flexibility is introduced and the whole system is co-simulated by using, on the one hand, the same multibody software dealing with the vehicle/track subsystem and,

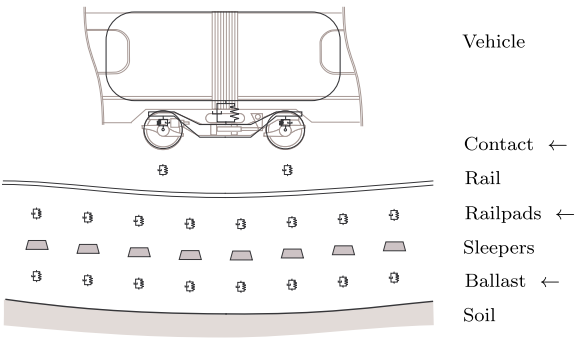

Fig. 1 Different places (denoted by "←") where the monolithic modeling vehicle/track/soil can be recoupled when using applied-force cosimulation techniques

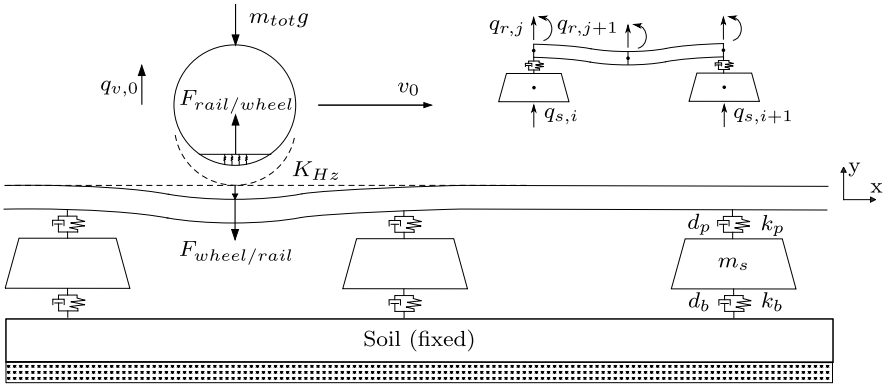

Fig. 2 Monolithic modeling of a single wheel rolling on a flexible track (rail – railpads – sleepers – ballast). Figure from [15]

on the other hand, a finite element code implementing the soil. In this case, the split takes place between the sleepers and the soil with a displacement/force coupling type, and for different types of soil (soft, medium, and stiff). Finally, the influence of the vehicle, either a simple wheel or a half-car is analyzed.

2 Model construction

The studied system is illustrated in Fig. 2. It consists of a railway vehicle moving on a flexible track. In this figure, the different degrees of freedom are identified by the letter q with the subscript v, r, and s for the vehicle, rail, and sleepers, respectively.

Two different parts will be presented in the paper depending on the nature of the soil:

Part 1. A study of the influence of the cosimulation approach, the data exchange time step and the type of coupling. For this part, the soil will not be considered.

Part 2. A study of the impact of the vehicle type and the soil flexibility on a more comprehensive model including a 3D finite element representation of the soil.

Through these two parts, the influence of the split location is also analyzed. Indeed, part 1 deals with the wheel/rail and railpads split cases, while part 2 is performed using a split located at the ballast level.

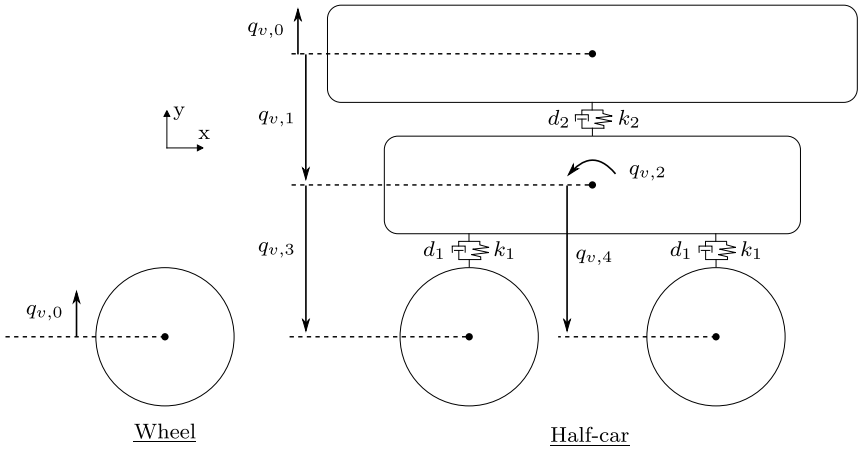

Fig. 3 Illustration of both vehicles used in the simulations

2.1 Subdomain definition

The entire system is basically composed of the four subdomains: vehicle, rail, sleepers, and soil. The subsystems used in the present cosimulated model are directly composed of these subdomains. The coupling elements between these subdomains, wheel/rail contact, railpads, and ballast may be used to recouple the subsystems since applied-force cosimulation techniques are used. Except for the soil, the vehicle, rail, and sleepers dynamics are modeled in 2D.

The vehicle is modeled in two dimensions using the minimal coordinates approach in multibody dynamics in an in-house software called EasyDyn [16]. It consists, initially, of a single wheel whose weight is equivalent to a regular wheel/rail static contact force $m_{\text{tot}}g$ in which the mass is taken as 10 t. This wheel, whose longitudinal motion is constrained to a uniform motion with a speed of 300 km/h, has therefore a unique vertical degree of freedom $q_{v,0}$. This simple model of the vehicle is used to isolate the vehicle and track behaviors while simulated using cosimulation techniques. Moreover, in this case, a monolithic reference is easily built by time-integrating all constitutive equations in a unique solver inside the multibody dedicated software. For a second description, the vehicle studied is considered as the half-car that has 4 bodies (two wheels, a bogie, and a part of the car) and whose motion is described by 5 degrees of freedom (the vertical motion of both wheels $q_{v,3}$ and $q_{v,4}$, the bogie $q_{v,2}$ and the car $q_{v,0}$ and the pitch of the bogie $q_{v,2}$). Both vehicles are illustrated in Fig. 3. Typical values of the springs ($k_1 = 6$ MN/m and $k_2 = 0.5$ MN/m) and dampers ($d_1 = 0.5$ kNs/m and $d_2 = 30$ kNs/m) are retained [17] for the suspensions. Moreover, the weight of the car was tuned so that the static force exerted between both wheels and the rail remains identical to that in the wheel case. The set of equations describing the vehicle motion can, generally speaking, be expressed by the residual Eq. (1) in which $\mathbf{q}_v$ is the vector of configuration parameters while the dotted and double-dotted versions are their first and second time derivatives, respectively; $\mathbf{M}_v$ contains the mass matrix of the system, $\mathbf{h}_v$ contains the Coriolis, gyroscopic, and centrifugal terms, and $\mathbf{g}_v$ represents a vector function of the external loads applied on the system:

$$\mathbf{M}_v(\mathbf{q}_v)\ddot{\mathbf{q}}_v + \mathbf{h}_v(\mathbf{q}_v, \dot{\mathbf{q}}_v) - \mathbf{g}_v(\mathbf{q}_v, \dot{\mathbf{q}}_v, t, \mathbf{f}_{\text{rail/wheel}}) = 0. \tag{1}$$

Table 1 Track parameters [17]

Component	Parameter	Symbol	Value	Unit
Rail	Section	A_r	63.8	cm^2
	Element length	L_r	0.3	m
	Geometrical moment of inertia	I_r	1987.8	cm^4
	Young's modulus	E_r	210	GPa
	Density	ρ_r	7800	kg/m^3
Railpads	Stiffness	k_p	180	MN/m
	Damping	d_p	28	kNs/m
Ballast	Stiffness	k_p	25.5	MN/m
	Damping	d_p	40	kNs/m

The rail is flexible and modeled by Euler–Bernoulli beam elements while the sleepers are modeled as rigid lumped masses (of 90.84 kg) with a single vertical degree of freedom. There are a distance of 0.6 m and two rail elements between the two sleepers. The extremities of the rail are not constrained and can move freely. However, the results will be observed when the vehicle is located approximately at the center of the track such that the effect of the rail extremities can be neglected. Knowing the material properties of the rail, its global mass $\mathbf{M}_r$ and stiffness $\mathbf{K}_r$ matrices can be established with respect to the degrees of freedom of the nodes depicted in Fig. 2. The different track parameters are concatenated in Table 1. If $\mathbf{q}_r$ designates the vector of rail configuration parameters and $\mathbf{g}_r$ the weight of the rail, the equations of motion of the rail are given in Eq. (2). For the sleepers, since they are modeled by vertically oscillating masses and since their flexibility is not taken into account, their dynamic behavior is given in Eq. (3), knowing that $\mathbf{q}_s$ is the vector sleeper vertical positions and $\mathbf{g}_s$ their intrinsic weight:

$$\mathbf{M}_r\ddot{\mathbf{q}}_r + \mathbf{K}_r\mathbf{q}_r - \mathbf{f}_{\text{wheel/rail}} - \mathbf{f}_{\text{sleepers/rail}} - \mathbf{g}_r = 0, \tag{2}$$

$$\mathbf{M}_s\ddot{\mathbf{q}}_s - \mathbf{f}_{\text{rail/sleepers}} - \mathbf{f}_{\text{soil/sleepers}} - \mathbf{g}_s = 0. \tag{3}$$

The railpads and ballast are modeled using spring–damper elements such that Eq. (4) gives the typical force between two nodes A and B (one rail node and one sleeper node, or one sleeper node and one soil point). In this equation, k and d can be replaced either by the stiffness k_b and damping d_b of the railpads or k_p and the damping d_p of the ballast to define the forces $\mathbf{f}_{\text{rail/sleepers}}$ or $\mathbf{f}_{\text{sleepers/soil}}$, respectively:

$$f_{\text{A/B}} = -f_{\text{B/A}} = -k\left(q_{\text{B}} - q_{\text{A}}\right) - d\left(\dot{q}_{\text{B}} - \dot{q}_{\text{A}}\right). \tag{4}$$

For the wheel/rail contact, a nonlinear Hertz contact defined by Eq. (5) is chosen, in which y_r denotes the vertical rail deflection at the contact point. The vertical deflection of the rail between the rail nodes is computed using polynomial shape functions proposed by Nielsen et al. [18], and the corresponding contact force is also distributed on the rail nodes using the same shape functions. In this equation the stiffness coefficient is $K_{\text{Hz}} = 92.86$ $\text{GN/m}^{\frac{3}{2}}$:

$$f_{r/v} = \begin{cases} K_{\text{Hz}}\left(y_r - q_{v,0}\right)^{\frac{3}{2}}, & \text{if } y_r - q_{v,0} > 0, \\ 0, & \text{otherwise.} \end{cases} \tag{5}$$

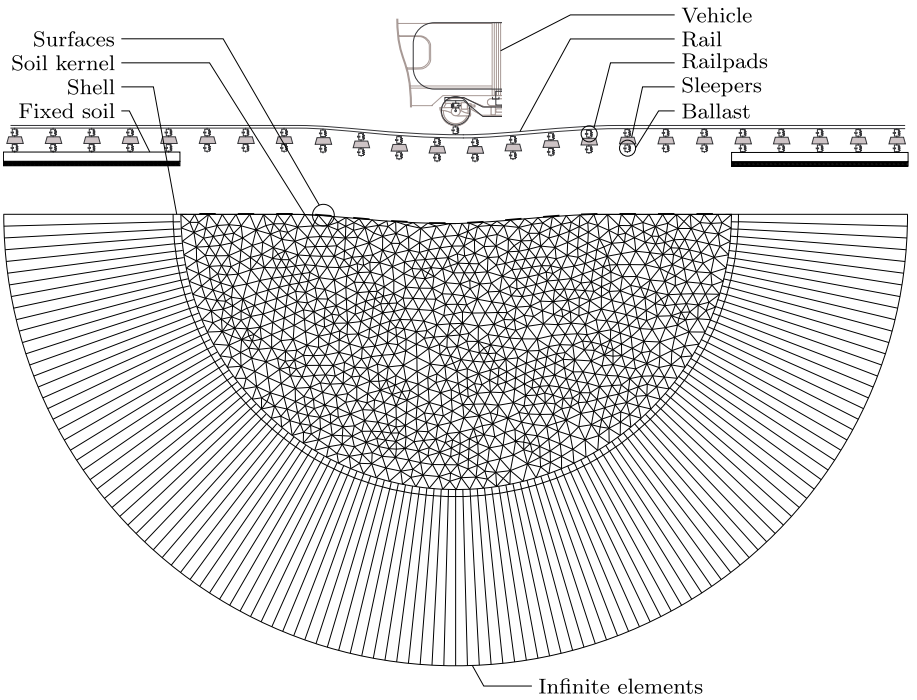

Fig. 4 Representation of the vehicle/track/soil including a three-dimensional modeling of the soil. Figure and model from [20]

When the soil is considered as flexible, a two-part and three-dimensional finite element modeling of a homogeneous soil is used (similar to the soil used in [19]). A commercial finite element software called Abaqus is used to model the entire soil. The modeling is represented in Fig. 4 and is described in [20]. The first part of this soil is a hemispherical kernel meshed with tetrahedral elements on which two tracks lay symmetrically with respect to the diameter of the hemisphere. The second part is a hemispherical envelope meshed with infinite elements so as to avoid undesirable wave reflection at the boundaries. Both parts are tied so that the soil kernel is not rigidly fixed to the bedrock. When the soil is considered as rigid, its corresponding configuration parameters and time derivatives are forced to 0 in Eq. (3) (at the level of force $\mathbf{f}_{\text{soil/sleepers}}$ computation). The considered soil is completely elastic and defined by its Young's modulus E, constant density (ρ = 1540 kg/m^3), constant Rayleigh proportional damping (β = 0.0004 s), and constant Poisson's ratio (ν = 0.25). Three different homogeneous soils are compared: soft (E = 10 MPa), medium (E = 155 MPa). and stiff (E = 750 MPa).

As illustrated in Fig. 4, the interaction between the three-dimensional soil and the two-dimensional track is performed through rigid surfaces defined on the soil surface. The center points of these surfaces are then linked to the sleepers through the ballast.

2.2 Subsystem definition

When the split location is known in a system, the composition of each subsystem is also known. However, in the present case, the split location is a studied point. Therefore, two subsystems are established as follows:

- *The upper subsystem* always contains the vehicle (either the wheel or the half-car). Depending on the split location, this subsystem will contain one or more elements of the track (rail and sleepers). The upper subsystem is always solved using the multibody dedicated software. The solver uses a Newmark-β scheme with tuned parameters such that it does not generate any artificial damping in the results. Moreover, the microtimestep of this subsystem is adaptive to provide a convergence even if the macrotimestep is too large.
- *The lower subsystem* consists of the soil and the parts of the track not included in the upper subsystem. When the soil is considered as rigid, it contains the sleepers only or the sleepers and the rail. In this specific case, the same solver as that used in the upper subsystem is employed. When the soil is considered as flexible, it contains only the soil, and the track is completely included in the vehicle subsystem. Meanwhile, the soil is time-integrated by an HHT-α scheme whose parameters are tuned to $\alpha = -0.05$, $\beta = 0.275625$, and $\gamma = 0.55$, which provides artificial damping for high frequency modes present in the soil due to its finite element modeling.

3 Coupling approaches

Applied-force coupling schemes are used to perform cosimulation in the present case. The split should therefore be performed at the level of an element through which a force is exerted. Since the wheel/rail contact, railpads, and sleepers are modeled as elastic elements, they can potentially be used to recouple the subsystems. The main advantage of this applied-force technique is to avoid algebraic constraints in the equations. The eligible coupling elements at which the system can be cut are indicated by an arrow in Fig. 1. Furthermore, once the split location is known (and thus the subsystems are defined), two main characteristics of the coupling must be detailed:

- *The coupling approach* being either Jacobi (denoted by J) or Gauß–Seidel (denoted by GS), that relates to the order of integration of the subsystems and also to the data management in between.
- *The coupling type* that defines the nature of the data exchanged between the subsystems. The nature of the coupling variables received by the subsystems are, in applied-force coupling, either a force quantity (denoted by T) or a kinematic quantity (denoted by X). When the elastic element through which both subsystems are coupled presents damping, the corresponding exchanged kinematic quantity must include the displacement and the velocity of the coupling point.

Both studied cosimulation approaches [21, 22] are illustrated in Fig. 5. In this figure, $\mathbf{z}$ denotes the concatenation of the state variables $\mathbf{z}_i$ of both subsystems, H denotes the macrotimestep, and $\mathbf{u}_i$ denotes the inputs of subsystems i at time t. The Gauß–Seidel scheme (Fig. 5a) consists of a sequential integration of both subsystems during a macrotimestep (timestep at which both subsystems exchange data) while Jacobi (Fig. 5b) is completely parallel. In the Gauß–Seidel scheme, the inputs $\mathbf{u}_1$ of subsystem 1 are functions of the state variables $\mathbf{z}_2^t$ computed at time t. For the second subsystem, however, the inputs $\mathbf{u}_2$ are functions of the state variables of subsystem 1 but after the micro-integrations of subsystem 1 over the macrotimestep. In the Jacobi approach, the integration of subsystem 1 remains similar to that detailed for Gauß–Seidel. This time, the inputs $\mathbf{u}_2$ of subsystem 2 are also functions of the state variables of subsystem 1 estimated at time t since both time-integration are performed in parallel. The actual communication between both subsystem is directly

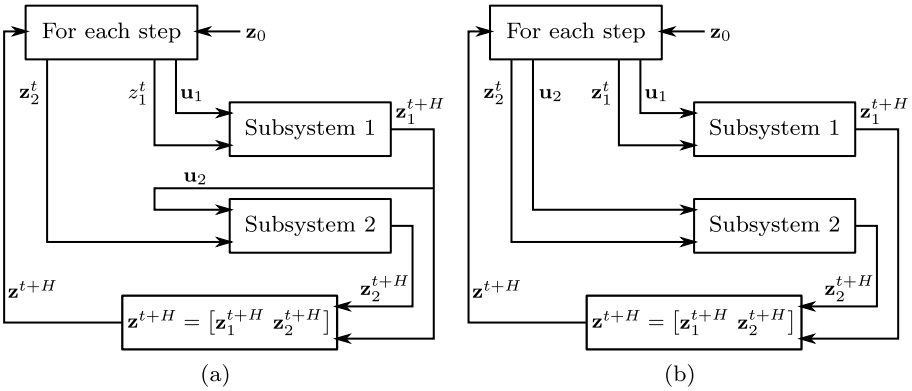

Fig. 5 Gauß–Seidel (left) and Jacobi (right) cosimulation schemes. Illustration of the loop over the macrotimesteps. Step procedure with initial conditions $\mathbf{z}_0$, subsystem i state variables $\mathbf{z}_i$, and subsystem i inputs $\mathbf{u}_i$. Figure from [24]

illustrated in the "For each step" cell in the figures, knowing that the drawings represent a loop executed over each macrotimestep. It is important to remark that no iterations are performed in either Jacobi or Gauß–Seidel approaches over the macrotimesteps. This directly influences the accuracy of the results but avoid an increase of the computational time. Since the sequential approach performs a first integration before integrating the second subsystem, the input values of the second subsystem, coming from the recoupling, are better estimates than the coupling values computed at the previous timestep. Therefore, with no iterations or predictive exchange of coupling variables, the sequential approach should be more accurate than the parallel one. When using iteration and extrapolation or predictive techniques in the exchange of coupling variables, this may be discussed [21, 23].

The coupling variables are exchanged in their trivial state, meaning that there is no explicit time-integration prediction while exchanging the data. Furthermore, there is no extrapolation or interpolation while performing micro-integrations inside each subsystem. These choices were made on purpose to highlight the effect of cosimulation approaches while changing the system parameters. Moreover, the iterations over macrotimesteps will considerably increase the computational burden when performing cosimulation with an actual finite element modeling of the soil which includes several hundreds of thousands degrees of freedom.

The coupling types used in this paper are the displacement/displacement and the displacement/force types denoted in this paper by X–X and X–T, respectively. Figure 6 illustrates an X–X coupling type with a split location at the level of the railpads (denoted R/S for Rail/Sleepers). In this case, both subsystems (S1 and S2, resp.) receive kinematic quantities ($\mathbf{u}_r$ and $\mathbf{u}_s$, resp.), from the other subsystem. They correspond to the displacement and velocity of the tip of the elastic coupling element which is not included in the considered subsystem. As both subsystem receive a kinematic quantity, the coupling element is explicitly represented in both subsystems. Here, the input values received by each subsystem are listed in Eq. (6a)–(6b) in which sleeper node i corresponds to rail node j and the curly braces symbolize a vector composed of all elements listed inside. In this case, the state variables $\mathbf{z}_1$ of subsystem 1 are the vehicle degrees of freedom $\mathbf{q}_v$, the rail degrees of freedom $\mathbf{q}_r$, and their first derivatives. In parallel, the state variables of subsystem 2 are the sleepers degrees of freedom $\mathbf{q}_s$ and the soil degrees of freedom (when its flexibility is taken into account) and

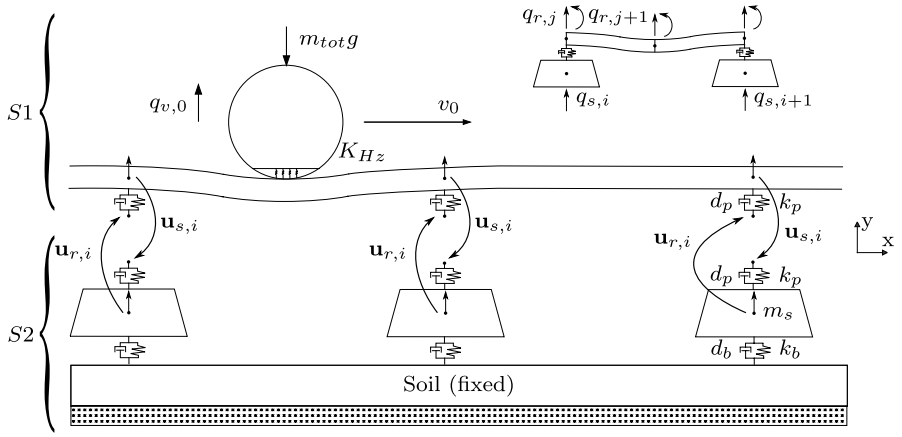

Fig. 6 A simple cosimulated modeling of a wheel, charged by a constant force $m_{\text{tot}}g$, moving on a track at a speed of v_0. The subsystems are $S1$ for the wheel and the rail, and $S2$ for the sleepers and the soil (fixed). They are split at the railpads level and recoupled using an X–X applied-force coupling type

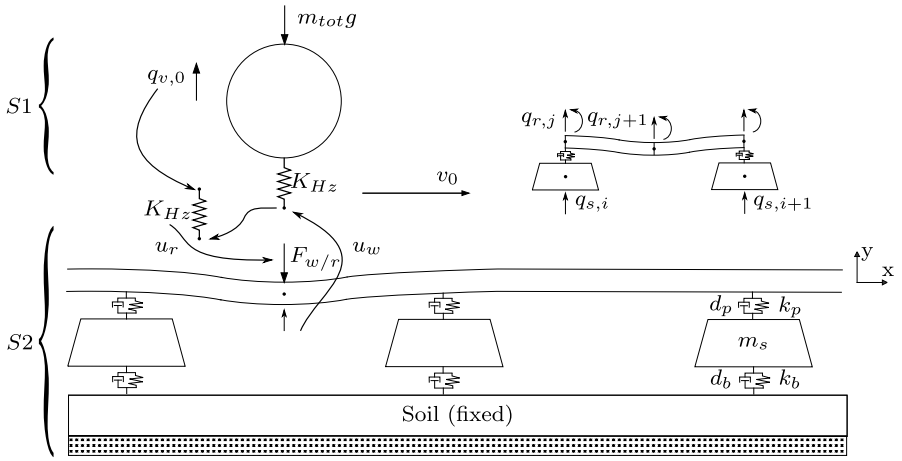

Fig. 7 A simple cosimulated modeling of a wheel, charged by a constant force $m_{\text{tot}}g$, moving on a track at a speed of v_0. The subsystems are $S1$ for the wheel only and $S2$ for the entire track. They are split at the contact level and recoupled using an X($S1$)–T($S2$) applied-force coupling type

their first time derivatives:

$$\mathbf{u}_r = \begin{bmatrix} \{q_{s,i}\} \\ \{\dot{q}_{s,i}\} \end{bmatrix}, \tag{6a}$$

$$\mathbf{u}_s = \begin{bmatrix} \{q_{r,j}\} \\ \{\dot{q}_{r,j}\} \end{bmatrix}. \tag{6b}$$

Figure 7 illustrates an X–T coupling type with a split location at the level of the wheel/rail contact (denoted W/R). In this case, the first subsystem receives a displacement u_w (no

damping) and the second receives $F_{w/r}$ the force applied by the other subsystem through the elastic element. It has to be mentioned that, in each coupling case, the inputs stay constant in each subsystem over a complete macrotimestep since there is no interpolation/extrapolation of the coupling variables in the considered cosimulation techniques. The state variables $\mathbf{z}_1$ of subsystem 1 are the vehicle degrees of freedom $\mathbf{q}_v$ and their first time derivatives. In parallel, the state variables of subsystem 2 are the rail degrees of freedom $\mathbf{q}_r$, the sleepers degrees of freedom $\mathbf{q}_s$ and the soil degrees of freedom (when its flexibility is taken into account) as well as their first time derivatives.

When the soil flexibility is not taken into account, a built-in cosimulation is implemented in the multibody dedicated software for test purposes. The co-simulation is therefore insured by a shared memory between the subsystems and the actual cosimulation manager is the main function of the C++ code. When the soil flexibility is taken into account, an actual cosimulation between EasyDyn and Abaqus is implemented as explained in [20]. In this case, the C++ code remains the master code, but everything is managed using a TCP/IP client–server communication.

4 Results

This section presents the results obtained for both parts considered:

- Firstly, the influence of the coupling approach, of the macrotimestep and of the coupling type through a simulation of a wheel rolling on a flexible track laying on a rigid soil.
- Secondly, the influence of the soil flexibility and vehicle type is investigated using X–T cosimulation between a vehicle/track subsystem and a three-dimensional soil subsystem. The used model [20] was depicted in Fig. 4.

In the following sections, when the soil is considered as rigid, the monolithic model corresponding to cosimulated situations is taken as the reference to demonstrate the effect of cosimulation techniques on the results. The monolithic reference is built by implementing all equations in the multibody dedicated software. The chosen macrotimestep for the monolithic reference is tuned to 10^{-6} s. They are therefore solved using the same and unique solver. When the soil flexibility is considered, the corresponding monolithic model cannot be easily established. Therefore, the results are compared with an already validated two-step model.

4.1 Coupling approach, type, and macrotimestep influence

In this section, the results obtained for a single wheel rolling on a flexible track and a rigid soil using various cosimulation implementations are compared with the monolithic modeling which is taken as a reference.

Figure 8 shows the rail deflection with respect to the track position at the specific time 0.2 s and with a macrotimestep of 10^{-4} s. This specific time corresponds approximately to the time for which the vehicle is located in the middle of the track. This was chosen to avoid as much as possible the side effects of the track modeling. Both coupling approaches are compared for a wheel/rail split location and for both X–X and X–T coupling types. It is clearly visible that for the same macrotimestep and coupling type, the Jacobi scheme can lead to abnormally amplified displacements while Gauß–Seidel does not. Moreover, in the Jacobi case, those abnormal oscillations appear only in the X–T case.

Figure 9 compares the coupling type and the split location through the error in the rail deflection with respect to the monolithic case. The observed time is identical to that in Fig. 8,

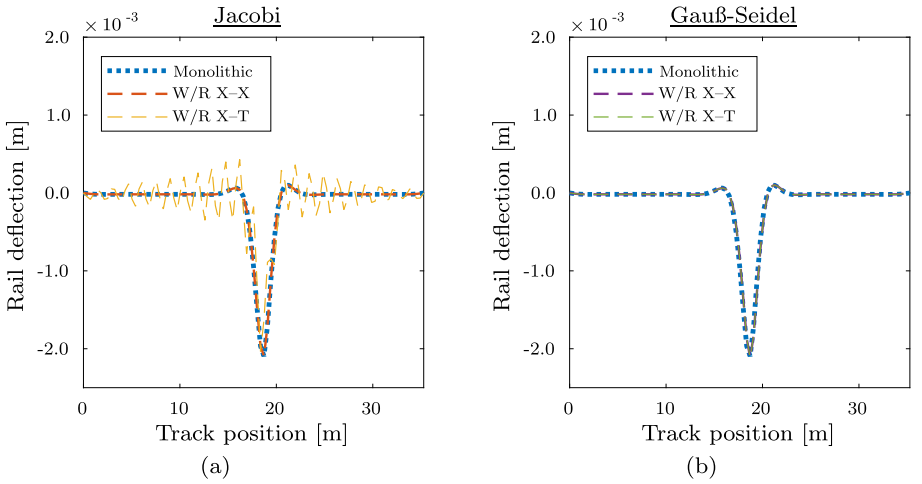

Fig. 8 Comparison of coupling approaches

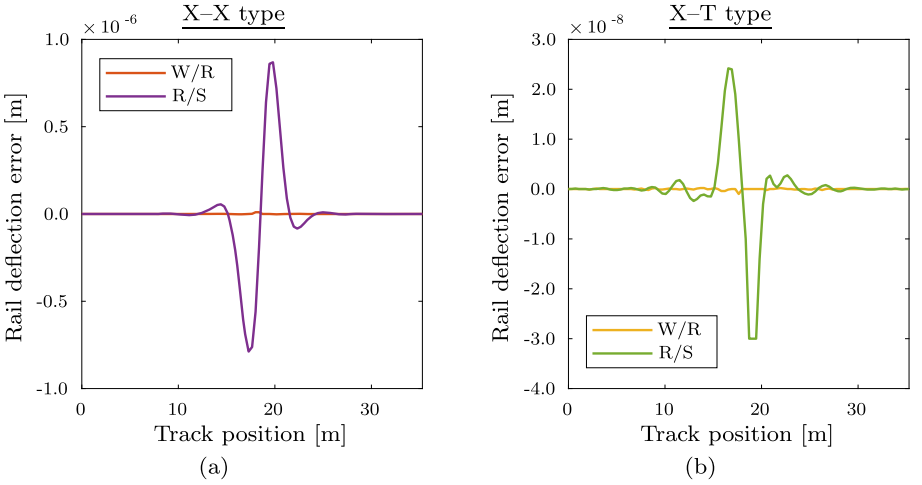

Fig. 9 Coupling type and split location comparison

the macrotimestep is taken as 10^{-6} s, and the coupling approach is only taken as Jacobi. In terms of the split location, it appears that the wheel/rail split stays more accurate than the rail/sleepers split for both coupling types. Moreover, the X–T case seems to be the most accurate coupling type.

Figure 10 illustrates the macrotimestep influence for different split locations and coupling types for the Jacobi coupling approach only. It clearly appears that the error converges to zero when the macrotimestep decreases.

Figure 11 shows the comparison between the error committed between the cosimulated models and the corresponding monolithic scheme for the rail and sleepers deflection. The Jacobi approach is used and the coupling is located at the railpads (R/S) level which means

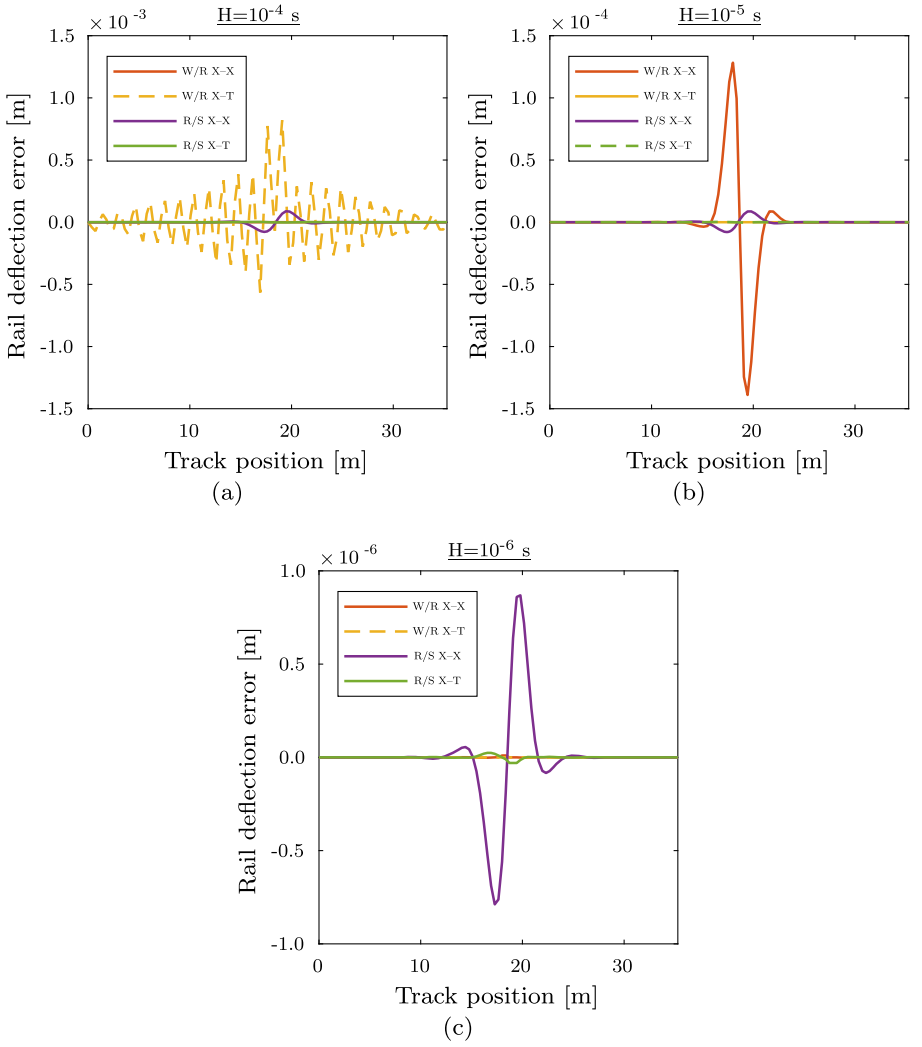

Fig. 10 Macrotimestep comparison

that the rail is included in the upper subsystem and the sleepers are included in the lower subsystem. The macrotimestep used is 10^{-4} s. In the X–T case, the error of sleeper deflection is bigger than the error of rail deflection while they remain comparable in the X–X type.

4.2 Soil flexibility and vehicle type influence

Since the ballast is modeled as independent spring and damper elements, each sleeper is connected to a rigid surface on the soil whose motion is reduced to the motion of a point. Figure 12 shows the vertical displacement of a point of the flexible soil corresponding to the 20th sleeper of a track with 81 sleepers. The macrotimestep is taken as 10^{-3} s, which is sufficient for the bandwidth observed in the present model. Moreover, taking a smaller

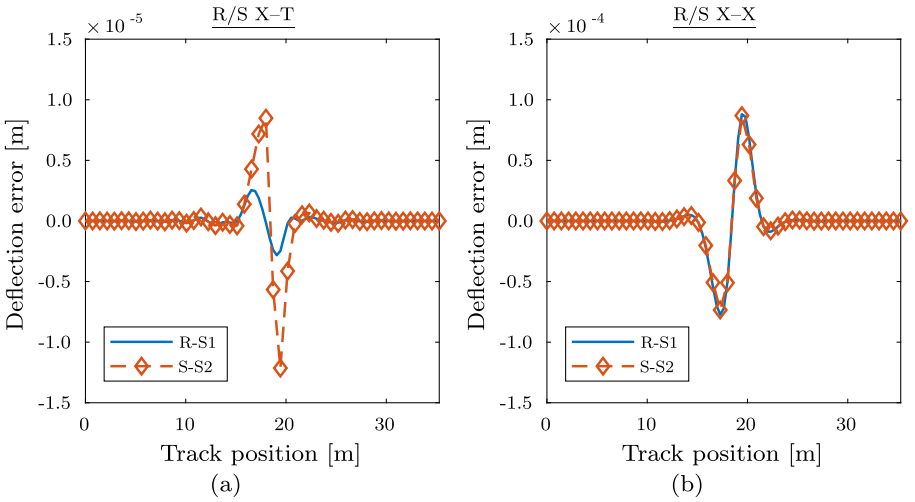

Fig. 11 Comparison between the rail and sleepers deflection error in the railpads cut (R/S) case. R-S1 denotes the rail in the upper subsystem and S-S2 the sleepers in the lower subsystem

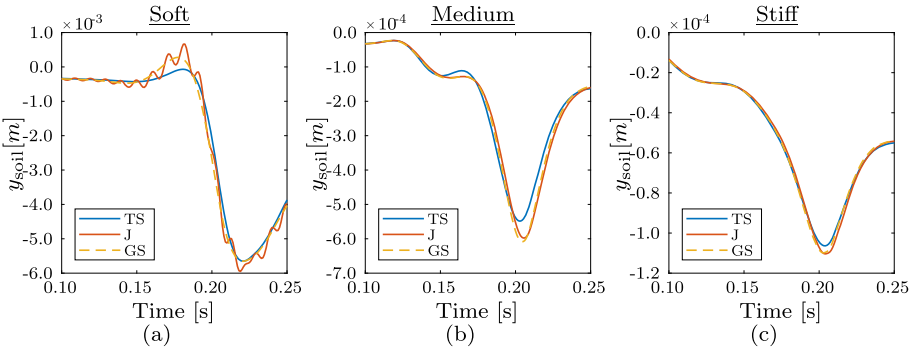

Fig. 12 Soil flexibility influence

macrotimestep considerably increases the computational burden. In each graph, the Jacobi (J) and Gauß–Seidel (GS) approaches are compared with a two-step (TS) and experimentally validated model [10, 19]. Generally speaking, it can be observed that the stiffer the soil, the closer the cosimulation results are to the two-step model. Moreover, in Fig. 12a, it can be seen that the Jacobi scheme presents abnormal oscillations while Gauß–Seidel does not.

Figure 13 compares two different vehicle types: a single wheel and a half-car, the rest of the model remaining identical. The vertical displacement of the same part of the soil as in Fig. 12 is observed and the same macrotimestep is taken. In each figure, the Gauß–Seidel approach is compared with the two-step model. For the half-car simulation, the maximal microtimestep (internal integration time step of subsystem) was voluntarily taken much smaller than in the wheel simulation for convergence purposes. Therefore, it is normal that the difference is smaller in the half-car case. However, the main drawback is a bigger simulation time.

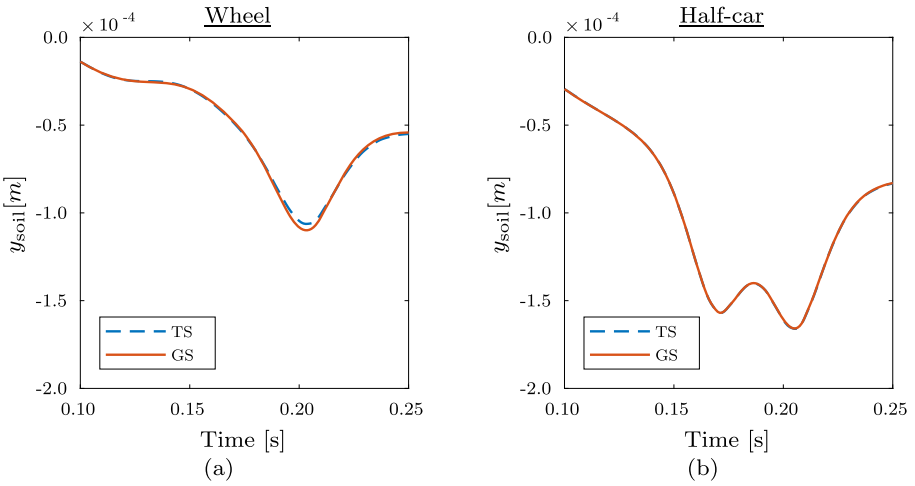

Fig. 13 Influence of the vehicle type on soil deflection

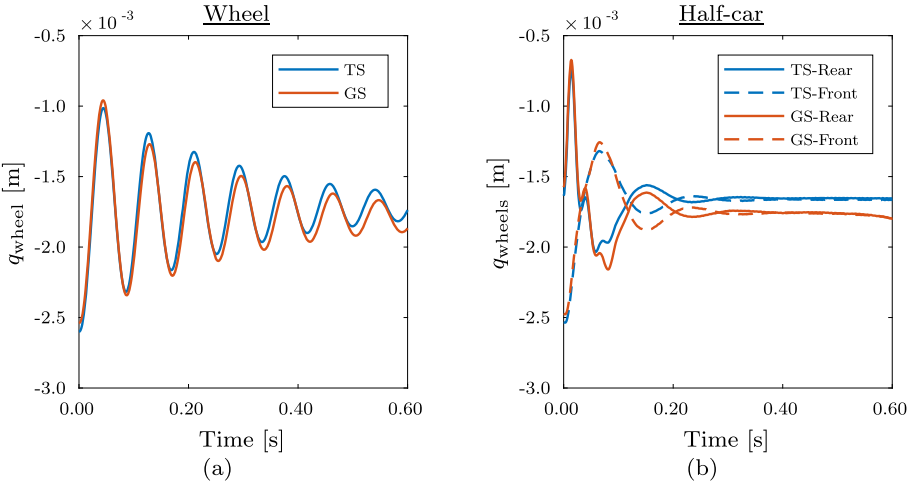

Fig. 14 Wheel motion in both types of vehicles

Figure 14 compares the wheel vertical motion for both types of vehicles. It can be seen that the order of magnitude remains the same for both types of vehicle. Moreover, for the half-car, it is clearly visible that the wheel motion is limited by the suspension effect while it is completely free in the single wheel vehicle. Furthermore, the comparison between the cosimulated models and the corresponding two-step model leads to the conclusion that the results are perfectly comparable either for the upper subsystem (corresponding to step one in the two-step model) or for the lower subsystem (corresponding to step 2 in the two-step model).

As stated in [20], the computational time required to perform the different simulation does not change between the different soil flexibilities. The most important parameter that

defines the computational burden of the presented model is the macrotimestep. In comparison with the two-step model, the sequential Gauß–Seidel approach takes up to 15% more time. This is justified by the time required to perform the communication between both programs and a more elaborated data management inside each solver which is a direct consequence of the cosimulation implementation. While using Jacobi (in stable cases only), the computational time is however reduced of approximately 15% since both programs works in parallel. This small difference between the two-step model and the cosimulated model using Jacobi is a consequence of the size of the soil model. Indeed, the soil includes several hundreds of thousands degrees of freedom and takes therefore the most important part of the computational time.

5 Conclusions

In case of multiphysics problems such as the vehicle/track/soil model, cosimulation constitutes a powerful technique to perform a simulation in which each subsystem is modeled in a convenient environment and is time-integrated using an adapted solver. After having briefly defined the cosimulated models used, this paper discussed the results obtained. Two different parts were discussed. The first part was a discussion on specific cosimulation options through a model including a rigid soil. The second part studied the soil flexibility and the vehicle influence with a more comprehensive model including a deformable soil. It was shown, through those comparisons, that the stability and the accuracy of cosimulated models depend on the cosimulation approach, the co-simulation type, the macrotimestep chosen and also the parameters of the system modeled.

Specifically for the vehicle/track/soil model treated in this paper, the following main characteristics can be established:

- As observed by Busch [21], using the sequential Gauß–Seidel approach provides more stable results than the parallel Jacobi approach.
- The coupling type exchanging only kinematic quantities (X–X) leads to less accurate results than the corresponding displacement–force (X–T) technique. Meanwhile, even if they are more accurate, the results obtained with the X–T type will comprise more oscillations and sometimes will be unstable (like in the W/R X–T case). This was also observed previously in the literature.
- Split the system at the railpads level may provide less accurate results than split at the wheel/rail contact level. However, cutting the system at the wheel/rail contact provides, in some cases, an unstable time-integration while the railpads cut does not. Further research must be performed on this point in order to find a proper indicator that qualifies the accuracy and stability of the different split locations.
- An irrevocable effect of the macrotimestep increase is an increase of the error committed on the results, no matter the split location, the coupling type or approach.
- When taking the soil flexibility into account, it appears that the softer the soil, the less accurate and less stable the results will be with respect to the two-step reference model.

It was observed that several cosimulation techniques used in this paper are not accurate and may present instability when the used macrotimestep is too large. However, large macrotimesteps are often sufficient to simulate the bandwidth of the observed phenomenon. Furthermore, large macrotimesteps are sometimes required to save computational time. A

perspective of the present work could be an investigation of the effect of explicit prediction of coupling variables and also extrapolation or interpolation over the microintegrations in order to improve the accuracy and the stability of the presented vehicle/track/soil model while keeping a sufficiently large macrotimestep.

References

1. Thompson, D.J., Kouroussis, G., Ntotsios, E.: Modelling, simulation and evaluation of ground vibration caused by rail vehicles. Veh. Syst. Dyn. **57**(7), 936–983 (2019)
2. Yang, J., Zhu, S., Zhai, W., Kouroussis, G., Wang, Y., Wang, K., Lan, K., Xu, F.: Prediction and mitigation of train-induced vibrations of large-scale building constructed on subway tunnel. Sci. Total Environ. **668**, 485–499 (2019)
3. Kouroussis, G., Verlinden, O., Conti, C.: On the interest of integrating vehicle dynamics for the ground propagation of vibrations: the case of urban railway traffic. Veh. Syst. Dyn. **48**(12), 1553–1571 (2010)
4. Alves Costa, P., Calçada, R., Silva Cardoso, A.: Vibrations induced by railway traffic: influence of the mechanical properties of the train on the dynamic excitation mechanism. In: De Roeck, G., Degrande, G., Lombaert, G., Müller, G. (eds.) 8th International Conference on Structural Dynamics: EURODYN 2011, Leuven (Belgium), pp. 804–811 (2011)
5. Zhai, W., Sun, X.: A detailed model for investigating vertical interaction between railway vehicle and track. Veh. Syst. Dyn. **23**(supplement), 603–615 (1994)
6. Zhai, W.M., True, H.: Vehicle-track dynamics on a ramp and on the bridge: simulation and measurements. Veh. Syst. Dyn. **33**(supplement), 604–615 (1999)
7. Kece, E., Reikalas, V., DeBold, R., Ho, C.L., Forde, M.C.: Evaluating ground vibrations induced by high-speed trains. Transp. Geotech. **20**, 100236 (2019)
8. Galvín, P., Domínguez, J.: Experimental and numerical analyses of vibrations induced by high-speed trains on the Córdoba–Málaga line. Soil Dyn. Earthq. Eng. **29**, 641–657 (2009)
9. Kouroussis, G.: Predicting High-Speed Railway Vibration Using Time-Domain Numerical Engineering Approaches pp. 187–216. ICE Publishing (2019)
10. Olivier, B., Connolly, D.P., Alves Costa, P., Kouroussis, G.: The effect of embankment on high speed rail ground vibrations. Int. J. Rail Transp. **4**(4), 229–246 (2016)
11. Antunes, P., Magalhães, H., Ambrósio, J., Pombo, J., Costa, J.: A co-simulation approach to the wheel–rail contact with flexible railway track. Multibody Syst. Dyn. **45**(2), 245–272 (2019)
12. Wu, Q., Spiryagin, M., Cole, C., McSweeney, T.: Parallel computing in railway research. Int. J. Rail Transp. **8**(2), 111–134 (2020). https://doi.org/10.1080/23248378.2018.1553115
13. Wu, Q., Sun, Y., Spiryagin, M., Cole, C.: Parallel co-simulation method for railway vehicle–track dynamics. J. Comput. Nonlinear Dyn. **13**(4), 041004 (2018)
14. Dietz, S., Hippmann, G., Schupp, G.: Interaction of vehicles and flexible tracks by co-simulation of multibody vehicle systems and finite element track models. Veh. Syst. Dyn. **37**(sup1), 372–384 (2002)
15. Olivier, B., Verlinden, O., Kouroussis, G.: A vehicle/track co-simulation model using easydyn. In: 7th International Conference on Computational Methods in Structural Dynamics and Earthquake Engineering, Hersonissos, Greece, pp. 1–10 (2019)
16. Verlinden, O., Fékih, L.B., Kouroussis, G.: Symbolic generation of the kinematics of multibody systems in EasyDyn: from MuPAD to Xcas/Giac. Theor. Appl. Mech. Lett. **3**(1), 013012 (2013)
17. Kouroussis, G., Verlinden, O., Conti, C.: Influence of some vehicle and track parameters on the environmental vibrations induced by railway traffic. Veh. Syst. Dyn. **50**(4), 619–639 (2012)
18. Nielsen, J.C.O., Abrahamsson, T.J.S.: Coupling of physical and modal components for analysis of moving non-linear dynamic systems on general beam structures. Int. J. Numer. Methods Eng. **33**(9), 1843–1859 (1992)
19. Kouroussis, G., Van Parys, L., Conti, C., Verlinden, O.: Using three-dimensional finite element analysis in time domain to model railway-induced ground vibrations. Adv. Eng. Softw. **70**, 63–76 (2014)
20. Olivier, B., Verlinden, O., Kouroussis, G.: A vehicle/track/soil model using co-simulation between multibody dynamics and finite element analysis. Int. J. Rail Transp. **8**(2), 135–158 (2020)
21. Busch, M.: Zur effizienten Kopplung von Simulationsprogrammen. Ph.D. thesis, Kassel University (2012)

22. Gomes, C., Thule, C., Broman, D., Larsen, P., Vangheluwe, H.: Co-simulation: a survey. ACM Comput. Surv. **51**(3), 49 (2018)
23. Busch, M.: Continuous approximation techniques for co-simulation methods: analysis of numerical stability and local error. Z. Angew. Math. Mech. **96**(9), 1061–1081 (2016)
24. Olivier, B., Verlinden, O., Kouroussis, G.: In: Schweizer, B. (ed.) Stability and Error Analysis of Applied-Force Co-Simulation Methods Using Mixed One-Step Integration Schemes. IUTAM Bookseries, vol. 35, pp. 243–254. Springer, Berlin (2019). Chapter 12